*HIPPOCAMPUS 19:855–868 (2009)*

# Electrical Signals Polarize Neuronal Organelles, Direct Neuron Migration, and Orient Cell Division

Li Yao,[1,2] Colin D. McCaig,[1*] and Min Zhao[1,3*]

**ABSTRACT: During early brain development, the axis of division of neuronal precursor cells is regulated tightly and can determine whether neurons remain in the germinal layers or migrate away. Directed neuronal migration depends on the establishment of cell polarity, and cells are polarized dynamically in response to extracellular signals. Endogenous electric fields (EFs) orient cell division and direct migration of a variety of cell types. Here, we show that cell division of cultured hippocampal cells (neuron-like cells and glial-like cells) is oriented strikingly by an applied EF, which also directs neuronal migration. Directed migration involves polarization of the leading neurite, of the microtubule-associated protein MAP-2 and of the Golgi apparatus and the centrosome, all of which reposition asymmetrically to face the cathode. Pharmacological inhibition of Rho-associated coiled-coil forming protein kinases (ROCK) and phosphoinositide 3-kinase decreased, leading neurite orientation and Golgi polarization in the neurons in response to an EF and in parallel decreased the directedness of EF-guided neuronal migration. This work demonstrates that the axis of hippocampal cell division, the establishment of neuronal polarity, the polarization of intracellular structures, and the direction of neuronal migration are all regulated by an extracellular electrical cue.** © **2009 Wiley-Liss, Inc.**

**KEY WORDS: electric fields; neuron; oriented division; directed migration**

## INTRODUCTION

Cell division plays an important role in development, wound healing, and pathology and the axis of cell division has major morphogenetic impact, for example, in shaping the developing cerebral cortex (Chenn and McConnell, 1995). During neurulation, maturation of the neural tube is associated with the transient appearance of spatially restricted small direct current electric fields (DC EFs) (Shi and Borgens, 1995). Their impact on neuronal cell division is untested. Later in brain development, once the decisions to polarize, divide asymmetrically, and leave the germinal zone have been made, neuroblasts subsequently migrate away from their place of birth and take up their final positions, for example, in the various laminae of the cerebral cortex. Directed neuronal cell division therefore is followed by directed neuronal migration and the cues regulating these processes are only partly understood. During directed cell migration, cells become polarized dynamically in response to extracellular directional signals. The polarized cell shape is characterized by membrane ruffling and filopodia at the front edge, reorientation of the microtubule-organizing center, and the Golgi apparatus in the direction of migration and coordinated reorganization of the actin cytoskeleton and microtubules (MTs) in the leading process (Nobes and Hall, 1999; Hayashi et al., 2003; Mellor, 2004; Tanaka et al., 2004).

Previous studies have shown that neurons steer their direction of migration using growth cone-like pathfinding and reorientation of the leading neurite (Yacubova and Komuro, 2002; Hayashi et al., 2003; Ward et al., 2003), with the Golgi and centosome located at the base of the leading neurite (Hayashi et al., 2003). In tangentially migrating neurons, nucleokinesis comprises several alternating phases: forward migration of the Golgi and centrosome into the leading neurite is associated with centrosome splitting and myosin contraction at the rear and nuclear translocation toward the displaced centrosome and Golgi apparatus (Bellion et al., 2005).

Previous findings suggested the involvement of electrical activity in pathfinding of growing axons and the formation of initial connections in the developing nervous system. Electrical activity influences the projection of growing thalamic axons toward their appropriate cortical target area (Catalano and Shatz, 1998) and axons of cortical pyramidal neurons to form layer-specific connections (Dantzker and Callaway, 1998). DC EFs also induce neurites to grow toward the cathode in culture (Jaffe and Poo, 1979; Hinkle et al., 1981; McCaig, 1986a,b), while also causing

[1] **School of Medical Sciences, University of Aberdeen, Aberdeen AB25 2ZD, Scotland, United Kingdom;** [2] **National Center for Biomedical Engineering Science, National University of Ireland, Galway, Ireland;** [3] **Department of Dermatology, University of California Davis, School of Medicine, California, CA 95618**

Additional Supporting Information may be found in the online version of this article.

Grant sponsor: Wellcome Trust: Grant numbers: 058551, 068012; Grant sponsor: British Overseas Research Student Award (ORS, Universities UK).

*Correspondence to: Min Zhao, Room 612D, Dermatology, Center for Neuroscience, UC Davis, School of Medicine, 1515 Newton Ct., Davis, CA 95618-4859, USA. E-mail: minzhao@ucdavis.edu or Colin McCaig, School of Medical Sciences, University of Aberdeen Aberdeen AB25 2ZD, Scotland, UK. E-mail: c.mccaig@abdn.ac.uk.

Accepted for publication 12 January 2009
DOI 10.1002/hipo.20569
Published online 11 March 2009 in Wiley InterScience (www.interscience.wiley.com).

retraction of neurites facing the positive pole (anode) (McCaig, 1987). However, although we were the first to show recently that neuronal migration was directed by a small applied EF (Yao et al., 2008), it is not known yet whether the EF can direct neuronal cell division and polarize the leading growth cone and intracellular structures (Golgi, centrosome, and MTs) to effect directed neuronal migration.

Rho family GTPases and phosphoinositide 3-kinase (PI3K) play a central role in establishing cell polarization, which involves asymmetric and ordered distribution of signaling molecules and of the cytoskeleton (Hannigan et al., 2002; Fukata et al., 2003). PI3K regulates the response of several cell types to EFs (Zhao et al., 2004; Pu and Zhao, 2005; Rajnicek et al., 2006). ROCK may cause neurite retraction (Hirose et al., 1998), although ROCK activity can also cause growth cone formation in cerebellar granule cells (Bito et al., 2000). During tangential migration of precerebellar neurons in response to netrin 1, ROCK inhibition causes axon extension and blocks neuronal migration (Causeret et al., 2004).

Here, we show that two key early events in neuronal development, oriented cell division and directed neuron migration are regulated by a small applied EF.

## MATERIALS AND METHODS

### Cell Culture

EFs were applied to neonatal hippocampal neurons using methods described previously (McCaig et al., 1994; Zhao et al., 1996). The final dimensions of the electrotaxis culture chambers in which cell division and migration occurred were 50 mm × 8 mm × 0.15 mm. Poly-L-lysine (100 μg/ml, Sigma, Dorset, UK) was applied to the central area of the dishes. After 2 h, the polyl-lysine solution was removed. Approximately 100 μl laminin (20 μg/ml; Sigma) (Yacubova and Komuro, 2002) was applied to the dried poly-L-lysine substratum overnight, at room temperature. Culture dishes prepared in this way were rinsed with culture medium before use.

Postnatal day P0-P3 rats were killed by cervical dislocation and then hippocampi were removed quickly from the skull and placed in Hepes-buffered saline (HBS). The tissue was washed in HBS and cut into tiny pieces. After this mechanical dissociation, the cultures contained many dissociated cells. Cells prepared in this way were seeded in the culture chamber dishes. Cultures were maintained in a humidified atmosphere of 5% $CO_2$ at 37°C.

### Electric Field Application and Administration of LY294002 and Y27632

After 12–18 h in culture, a DC EF (50–300 mV/mm) was applied to the cultured hippocampal cells. Agar-salt bridges (Steinberg's solution gelled with 1% agar) not less than 15-cm long were used to connect silver–silver chloride electrodes in beakers of Steinberg's solution to pools of excess culture medium at either side of the chamber. Culture conditions for control experiments were identical, except no EF was applied. For pharmacological inhibition experiments, neurons were pretreated with medium containing LY294002 (50 μM) or Y27632 (10 μM) for 1 h, then exposed to EFs in the continued presence of the inhibitor.

### Time-Lapse Microscopy

Neurons were observed with a Zeiss Axiovert 100 or Nikon 300 microscope with Hoffman modulation condenser and objective lenses (10×, 20×, 32×, 40×). Time-lapse experiments were performed using a MetaMorph 6.1 imaging system with a motorized X, Y, Z stage (Universal Imaging Corporation, Downingtown, PA). The temperature was maintained at 37°C during the experiments by using a microscope stage incubator. Sterile conditions were maintained throughout.

The position of each cell at $t = 0$ is represented by the origin (0, 0) (Figs. 4J,K and 5B), with the final position of each cell at 1 h plotted as a single point on the graph. The radius of each circle represents 100 μm.

### Cell Division Studies

Cell division was recorded and quantified using time-lapse video microscopy. At the end of the recording of cell division, cells were fixed with 4% paraformaldehyde, and immunostained with anti-MAP-2 antibody and anti-GFAP antibody to determine the neuronal cell type.

### Immunocytochemistry

Hippocampal neurons were fixed with 4% paraformaldehyde (20 min) and permeabilized with 0.2% Triton X-100 (10 min). Cells were exposed to blocking solution (10% serum, 1% BSA) for 20 min. All antibodies were diluted in PBS with 1% BSA. Hippocampal cell cultures were incubated with monoclonal primary antibody anti-MAP-2 (1:500, Sigma) or polyclonal primary antibody anti-MAP-2 (1:200, Sigma) for 1 h at room temperature.

Centrosomes were stained with Pericentrin rabbit polyclonal primary antibody (1:150, Covance, Berkeley, US) for 1 h. After washing, cells were incubated with Texas red conjugated antirabbit secondary antibody [Goat antirabbit Texas-red (1:100, Jackson, Suffolk, UK] for 50 min. The Golgi apparatus was labeled with GM130 mouse monoclonal primary antibody (1:100, BD Transduction Laboratories, Oxford, UK) for 1 h. After washing, cells were incubated with FITC conjugated antirabbit secondary antibody Donkey antimouse ALEXA 488 (1:200, Molecular probe, Paisley, UK) for 50 min. Nuclei were stained with DAPI.

### Cell Polarity Analysis

To quantify neuronal polarization, the neuronal cell body was divided into quadrants as shown (Fig. 4I). The blue line outlines the leading process/growth cone and growth cone

orientation was assessed by counting the percentage of growth cones that projected into the cathode-facing quadrant (C in Fig. 4I), that is, those that projected at angles between 45° and 315° to the EF vector, which runs horizontally between 180° and 360°. This criterion was also used for scoring polarization of Golgi and centrosomes. Because this analysis involves equal quadrants, random polarization of organelles would result in scores of 25% in each quadrant. The percentage of polarized cells ± s.e.m was calculated from at least three separate experiments.

The distribution of MAP-2 staining was determined by analyzing the fluorescent intensity using the linescan function in Metamorph software. The analysis method is similar to that used previously (Zhao et al., 2002). A single cell was divided into a cathodal half and an anodal half by a line perpendicular to the EF vector and through the center of the cell. The distribution of MAP-2 staining was categorized as cathodal asymmetry, anodal asymmetry, or symmetrical distribution from analysis of the linescans.

To determine the orientation of the neurite extending from the leading edge, a neurite orientation index was calculated for each time point and field strength. The alignment of the leading neurite was measured by drawing a line between the point at which the process emerged from the soma and the center of the neurite growth cone (Rajnicek et al., 1992). The angle between the axis of the neurite process and the line of the EF vector is α. The orientation index is the cosine of the angle α. If neurite alignment was parallel to the EF vector and facing the cathode, then $\alpha = 0$ and the orientation index will be 1. If neurite alignment was parallel to the EF vector and facing the anode, then $\alpha = 180$ and the orientation index will be −1. To quantify the average directedness of neurite orientation, the cosine values were averaged using the formula, $\cos \alpha = \Sigma i \cos \alpha i/N$, where $\Sigma i$ = summation of cosine values obtained from individual cells from at least three experiments at a given EF strength, α is the angle between the field axis and the direction of neurite orientation, and $N$ is the total number of cells contained in all of the experiments at that field strength (Fig. 7E).

### Statistics

Statistical analysis was made using paired *t*-test or unpaired, two-tailed Student's *t*-test. Data are expressed as mean ± s.e.m., unless stated otherwise.

## RESULTS

### Electrical Signals Orient the Cleavage Plane of Cell Division in Cells From Neonatal Rat Hippocampus

Anti-MAP-2 antibody is widely accepted as a neuron-specific marker and labels early neurite outgrowths of hippocampal neurons (Kwei et al., 1998; Miyata et al., 2003). We labeled cultured neonatal hippocampal cells with anti-MAP-2 antibody and anti-GFAP antibody. Two clearly different cell morphologies were seen (Fig. 1). Most neuone-like cells (MAP2-stained) were bipolar in shape and migrated with a leading growth cone-like structure. Dissociated glial-like cells (GFAP-stained) had a flat and irregular morphology, usually with multiple outgrowths. Both cell types divided in culture and when exposed to an applied EF, both cell types showed oriented cell division. Figure 2 shows cell divisions with and without EFs application, respectively. The neuronal phenotype of the daughter cells after division was determined by immunostaining with anti-MAP-2 antibody.

To further analyze the effect of EFs on the plane of cell division, the cleavage plane of the dividing cells was outlined as shown in Figures 2A,B. To quantify the orientation angle of the cleavage plane relative to the EF vector, the cell divisions were expressed as a polar diagram, where each dot represents the cleavage plane of one cell (Figs. 3A,B). Angles of cleavage plane of 28 dividing cells cultured without EFs and of 21 cells in a small physiological EF (between 50 and 300 mV/mm) were measured. A mean oriented division index was calculated using the angles measured for each cleavage plane. This was done by using the equation $\Sigma n \cos [2 (\theta\text{-}90^\circ)]/n$ (Zhao et al., 1999). For example, if all cells divide perpendicular to the EF vector (i.e., at an angle of 90°), then cos [2(90°-90°] becomes cos 0° that gives an oriented division index of 1. Alternatively, if the cleavage planes all lay at an angle of 0° that is parallel to the EF vector, then the cos [2(0°-90°] becomes cos −180° with an oriented division index of −1. Randomly oriented cell divisions should give an overall cleavage plane angle around 45° and an oriented division index of 0. The oriented division index of control cells was around 0 (0.0 ± 0.1) (Fig. 3C), however, the cells exposed to a small EF had a strong oriented division index of 0.5 ± 0.1 (Fig. 3C) ($P < 0.01$). Clearly, a high proportion of cells divide with a cleavage plane orthogonal to the EF, and with their mitotic spindle oriented parallel to the EF vector.

### Electrical Signals Direct Polarization of Neonatal Hippocampal Neurons

The morphology and identity of hippocampal neurons was demonstrated using neuronal markers (anti-MAP-2 antibody). For most MAP-2 positive cells, the overall shape of the cells was bipolar with a leading growth cone process and elliptical cell somas. This neuronal morphology is the same as reported previously (Edmondson and Hatten, 1987; Rickmann et al., 1987, Dotti et al., 1988; Gasser and Hatten, 1990; Bradke and Dotti, 2000). Only cells with this typical morphology were selected in the neuron polarization and neurite reorientation studies.

In an applied EF of 300 mV/mm, hippocampal neurons became polarized with the leading process/growth cone facing the cathode (Figs. 4A–C, Yao et al., 2008). Exposure to an EF of 300 mV/mm for 1 h resulted in 62.7% ± 3.2% ($n = 56$) of cells showing distinct polarized leading neurite morphology,

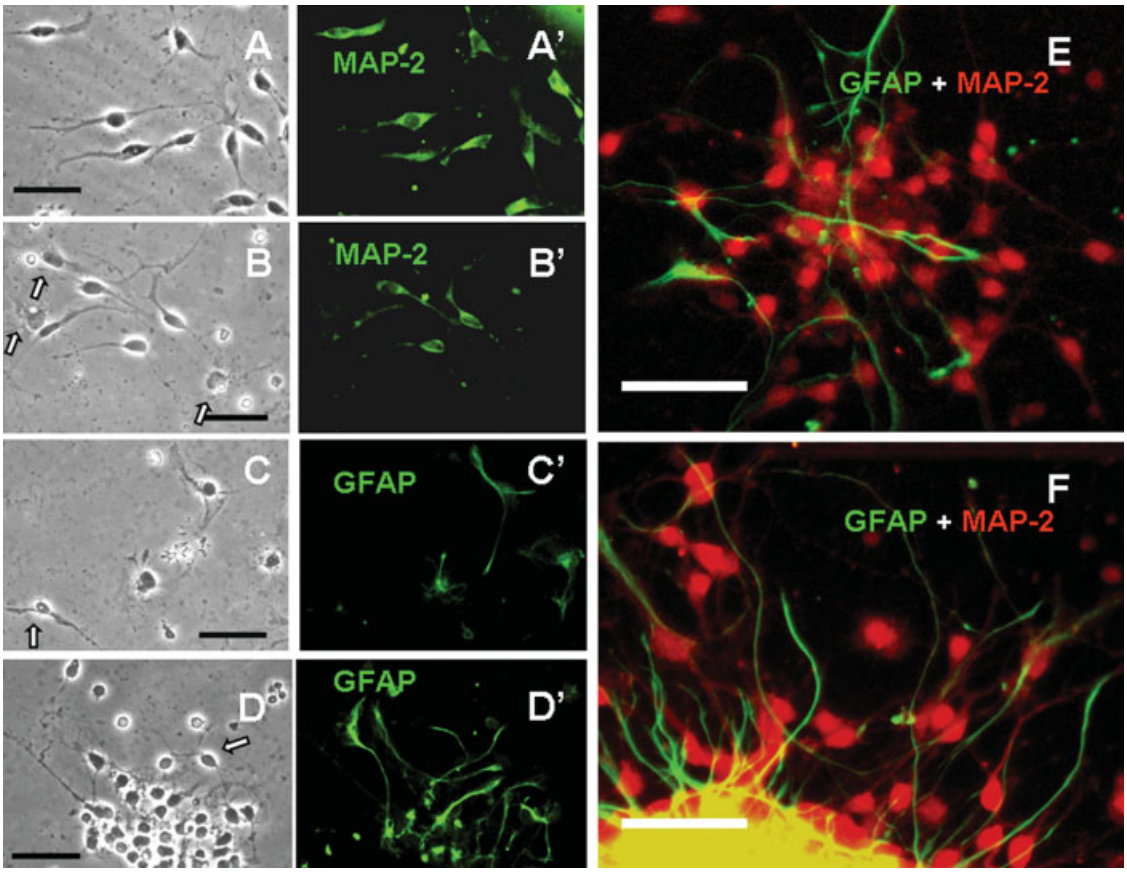


**FIGURE 1. MAP-2 and GFAP staining of hippocampal cells at early stage cell culture. (A, A', B, B') Neuron extended short neurites and were stained with MAP2 in early culture. Cells with flat and irregular morphology were not stained with anti-MAP-2 antibody (white arrows labeled cells). (C, C') The cells with flat and irregular morphology were stained with GFAP. Neuron with the bipolar shape was not labeled with anti-GFAP antibody (arrow labeled cell). (D, D') GFAP staining. When the glial cells were located among the neurons, they showed elongated shapes. However, the morphology of the elongated glial cells is very different from the bipolar neurons. The arrow indicated the nonstained neuron-like cell. (E) Dual labeling with anti-MAP-2 antibody and anti-GFAP antibody showed the elongated morphology of glial cells (green) in the neuron (red) micro-aggregate. (F) The glial cell processes (stained with GFAP, green) extended out of the hippocampal micro-explant, while the neurons (stained with MAP-2, red) migrated out of the explant. Scale bar, 50 μm. [Color figure can be viewed in the online issue which is available at www.interscience.wiley.com.]**

significantly higher ($P < 0.01$) than that in control cultures without an applied EF (28% ± 2%, $n = 49$) (Fig. 4L).

We used immunostaining to reveal the location of the Golgi apparatus and centrosome and their relationship with the nucleus. In hippocampal neurons cultured in an applied EF of 300 mV/mm, both the Golgi apparatus and the centrosome became polarized toward the cathode, whereas in cells cultured without an applied EF, the Golgi apparatus and centrosome were positioned randomly (Figs. 4E–H). After EF application, the percentage of Golgi apparatus lying in the cathode-facing quadrant was 56.9% ± 2.1% ($n = 128$), which is significantly higher than control (no EFs 28.5% ± 2.6%, $n = 96$, $P < 0.01$). 58.4% ± 2.9% ($n = 72$) of centrosomes in hippocampal neurons cultured in 300 mV/mm were also polarized toward the cathode, compared to the random centrosome positioning seen in control neurons (24.5% ± 2.7%, $n = 82$; $P < 0.01$).

In agreement with our previous study (Yao et al., 2008), an applied EF of 100–300 mV/mm promoted cathode-directed migration of hippocampal neurons, while neurons migrated randomly without EF stimulation. Here, 64.9% ± 6.9% ($n = 56$) of the cells migrated into the cathode-facing quadrant (between 45° and 315°) in EF (Fig. 4K), which is significantly higher than in controls without EF stimulation (30.7% ± 3.9%, $n = 49$) (Fig. 4J).

## PI3 Kinase and ROCK Signaling Are Essential in Establishing Neuron Morphology and Golgi Polarization

To study the role of PI3K and ROCK on neurite orientation in EFs, hippocampal neurons were pretreated with a PI3K inhibitor (LY294002) and with a ROCK inhibitor (Y27632) before being exposed to the EF. After treating with LY294002

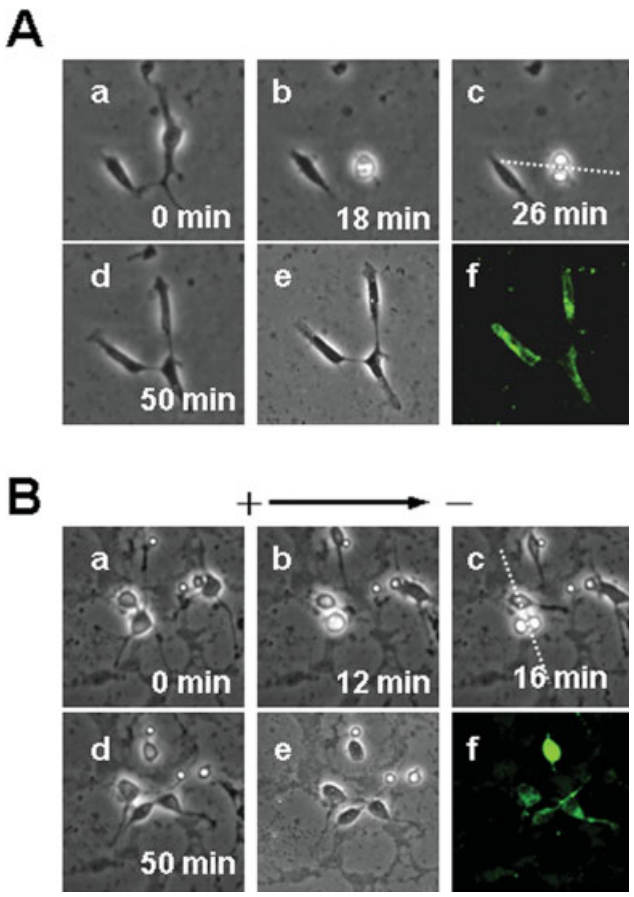


**FIGURE 2. Cell division in EFs. Cell division was recorded using time-lapse imaging. (A) A cell dividing without EFs application. (B) A cell dividing in an applied EF of 300 mV/mm. White dashed lines are drawn in A(c) and B(c) to highlight the cleavage planes of neuronal cell division. At the end of the experiments, the cells were fixed with 4% paraformaldehyde. A(e) and B(e) are the images showing the cells after fixation. The daughter cells after division are labeled with the neuron-specific anti-MAP-2 antibody. See also Supporting Information Videos 1.1 and 1.2. [Color figure can be viewed in the online issue which is available at www.interscience.wiley.com.]**

(50 μM) and an EF, only 34.4% ± 4.4% of the cells showed polarized morphology, which is significantly lower than in EF-exposed neurons with no drug ($P < 0.01$). After treating with Y27632 (10 μM) and an EF, 37.4% ± 4.1% of the cells showed polarized morphology, which again is significantly lower than in EF-exposed neurons with no drug ($P < 0.01$) (Fig. 5B).

Both LY294002 and Y27632 also reduced Golgi polarization significantly in EFs ($P < 0.01$). After exposure to LY294002 (50 μM), the percentage of neurons with cathodally polarized Golgi was decreased to a random value of 26.3% ± 2.4% ($n = 84$; compared to 57% in EF alone) and exposure to Y27632 (10 μM), induced a similar reduction to 33.3% ± 2.6% ($n = 95$; compared to 57% in EF alone). Neither was significantly different from the random orientation of 25% expected from cells with no EF exposure (Fig. 5C).

## Electrical Signals Direct Asymmetric Distribution of MAP-2 in Hippocampal Neurons

To determine the distribution of neuronal MTs in neurons exposed to an applied EF, neurons were stained with MAP-2. Both phase contrast bright field images and fluorescent staining images were taken to show cell morphology and the distribution of MAP-2. An asymmetric distribution of MAP-2 between leading and trailing neurites has been seen in cultured neurons. This asymmetric distribution is observed in both neurons with

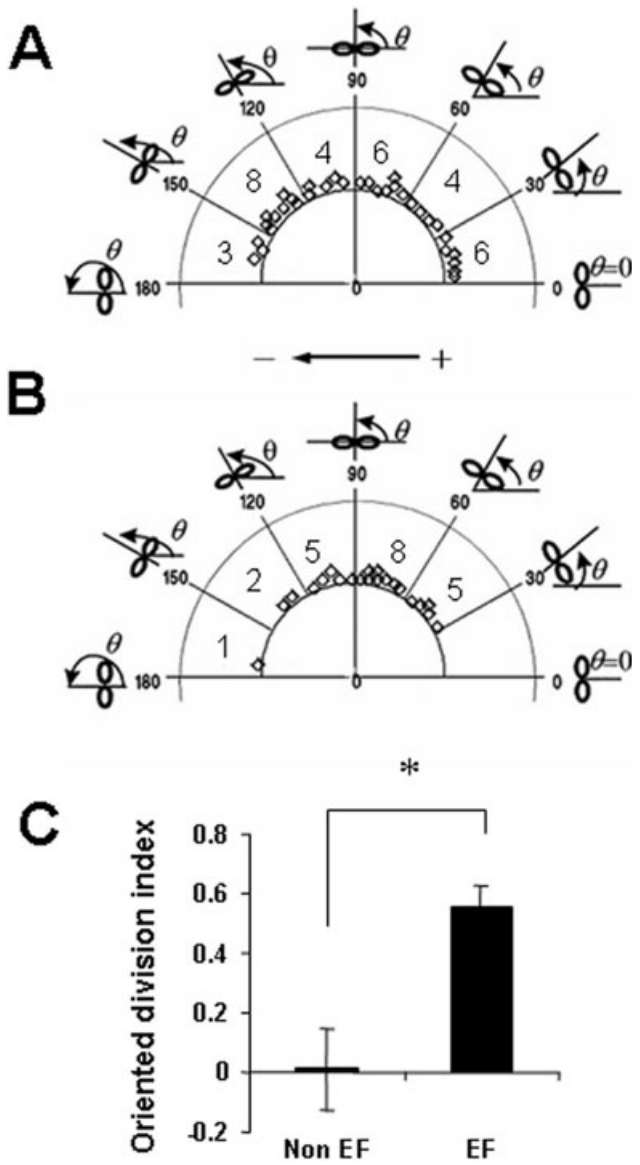


**FIGURE 3. Analysis of effect of EFs on cell cleavage plane. Angles of cleavage plane of rat hippocampal neurons were expressed as a polar diagram, where each symbol represents one cell. Cell division was followed with time-lapse recording. (A) Angles of cleavage plane of 28 dividing cells cultured without electric fields. (B) Polarized orientation of the cleavage plane of 21 cells dividing in a small EF (between 50 and 300 mV/mm). (C) Mean oriented division index of cleavage plane (see Results section and Zhao et al., 1999). *$P < 0.01$.**

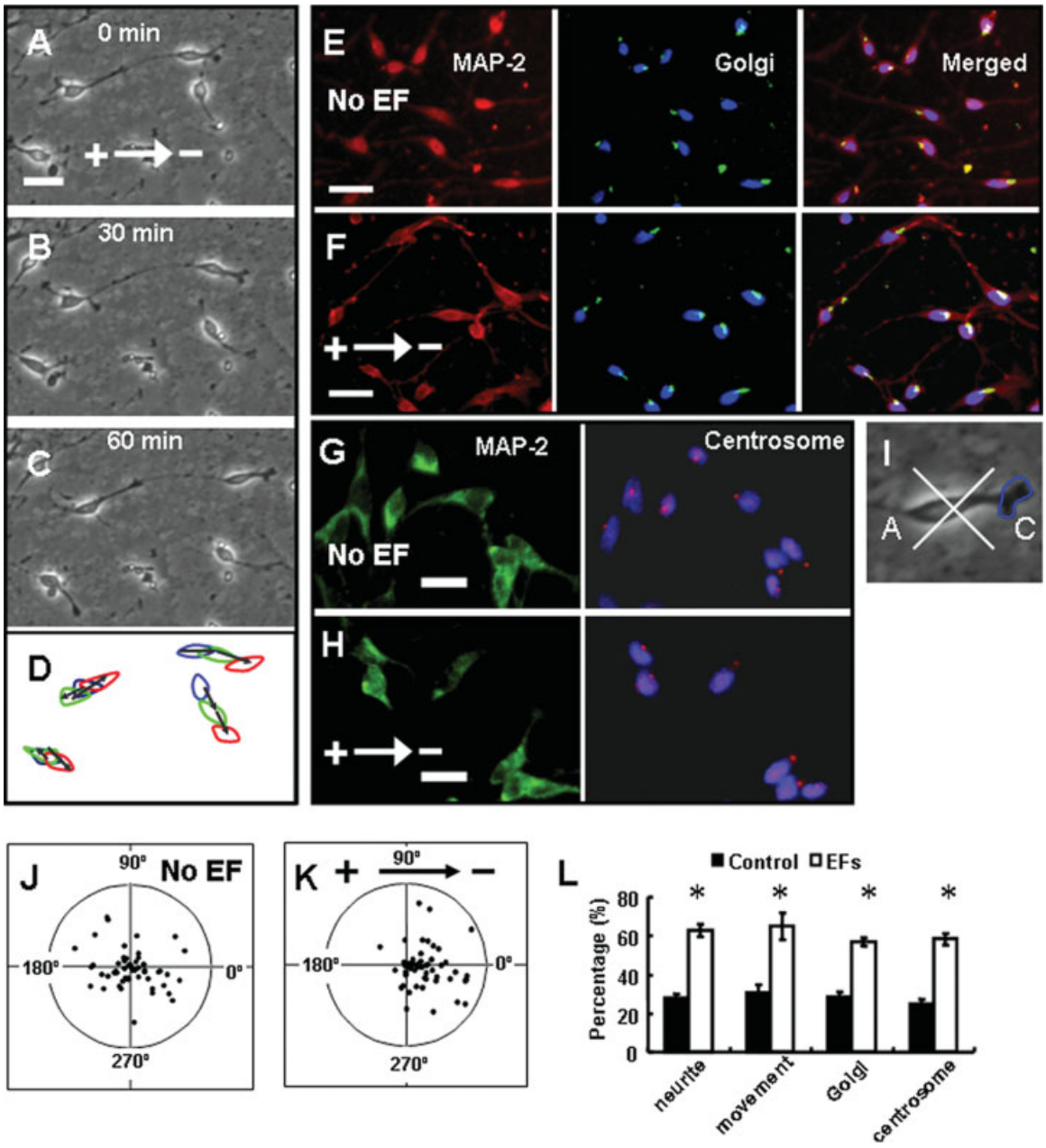


**FIGURE 4.** Electric fields induce cathodal polarization of hippocampal neurons. (A–C) Time-lapse images show cathodal orientation of leading neurites and cathode-directed migration of hippocampal neurons in a DC EF (300 mV/mm for 60 min). Scale bar: 30 μm. (D) Colored outlines of the four cell somas from A–C track the cathodal-directed migration of neurons (black arrows). Blue: 0 min; Green: 30 min; Red: 60 min. Positioning of Golgi (green) in rat hippocampal neurons cultured in the absence (E) or presence (F) of an applied EF for 1 h. Cells were triple-labeled with MAP-2 antibody (red), GM130 antibody (Golgi marker, green), and DAPI (blue). In (F), Golgi is polarized to the cathode at right. Scale bar: 30 μm. (G) and (H) Distribution of centrosome in neurons cultured in absence or presence respectively of an applied EF for 1 h. Centrosomes are polarized cathodally (to the right in H). Hippocampal neurons were labeled with anti-Pericentrin antibody (red), DAPI (blue), and anti-MAP-2 antibody (green). Scale bar: 20 μm. (I) Diagram shows the neuronal cell body divided into quadrants. The blue line outlines the growth cone on the leading process of a migrating neuron that is almost entirely in the cathode-facing sector. A, anodal quadrant; C, cathodal quadrant. (J, K) Neurons migrate cathodally in an EF (300 mV). The position of each cell at $t = 0$ is represented by the origin (0, 0), with the final position of each cell at 1 h plotted as a single point on the circular plot. The radius of each circle represents 100 μm. In J, control neurons (no EF) migrate in random directions and in K migration is directed cathodally. (L) Analysis of neuron polarization. The percentage of growth cone, Golgi, and centrosome falling in the cathode-facing quadrant (see I above) in neurons stimulated with EFs is significantly higher than in control neurons (no EF). $^*P < 0.01$. [Color figure can be viewed in the online issue which is available at www.interscience.wiley.com.]

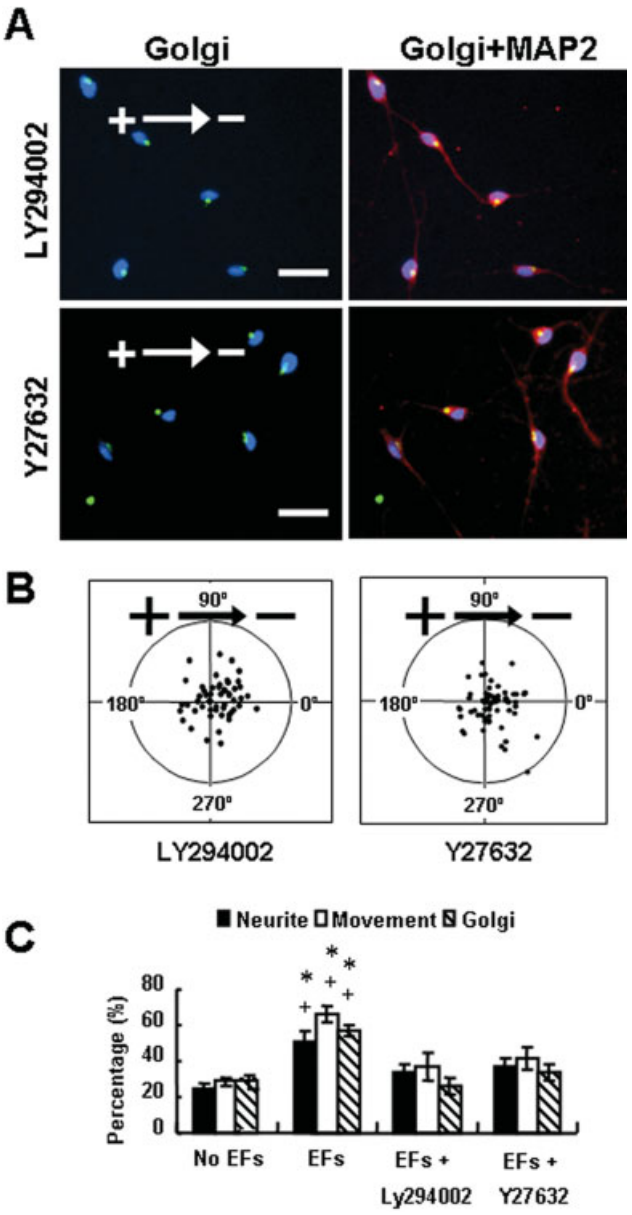


**FIGURE 5.** **ROCK and PI3K signal EF-induced neuron polarization and migration. (A) The normal cathodal polarization of the Golgi in an applied EF (compare with Fig. 1F) was disrupted in cells exposed to either LY294002 or Y27632. (B) The net translocation of neurons pretreated with LY294002 or Y27632 in an EF. Cells treated with either LY294002 or Y27632 showed markedly inhibited cathodal neuronal migration in the EF (compare with Fig. 4K). (C) Analysis of neuronal migration, polarization of growth cone, and Golgi polarization. *$P < 0.01$ when compared with the no EF group; +, when compared with the EF drug-pretreated group. Scale bar: 30 μm. [Color figure can be viewed in the online issue which is available at www.interscience.wiley.com.]**

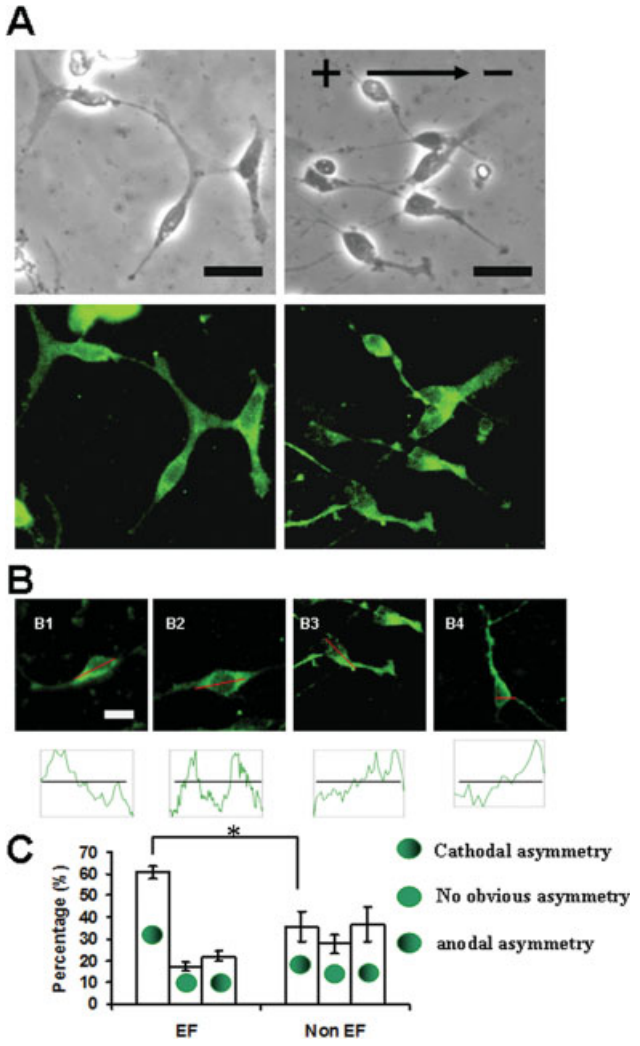


**FIGURE 6.** **An applied EF induced asymmetric distribution of MAP-2 in migrating hippocampal neurons. (A) Rat hippocampal neurons were labeled with anti-MAP-2 antibody (green). After being stimulated with EFs (300 mV/mm) for 1 h, neurons oriented with their leading process facing the cathode. MAP-2 staining was more intense at the cathode side of neurons. Scale bar: 25 μm. (B) The distribution of MAP-2 in neurons in the absence (B1, B2) or presence of an EF (B3, B4). Linescans of fluorescent intensity for each cell are shown. (B1) Asymmetrical distribution of MAP-2 along long axis of the neuron. (B2) No obvious asymmetrical distribution of MAP-2 was seen along the long axis of the neuron. (B3) Asymmetrical distribution of MAP-2 along the long axis of the neuron. (B4) Asymmetrical distribution of MAP-2 along the cross section of the neuron. Scale bar: 15 μm. (C) Analysis of asymmetrical distribution of MAP-2 in migrating neurons steering cathodally in an EF. Percentage of cells showing MAP-2 cathodal asymmetry (higher fluorescent intensity at the right or cathode facing side), anodal asymmetry (higher fluorescent intensity at the left or cathode facing side), and no asymmetry are shown in graph. The cathodal asymmetry of MAP-2 in EF-directed migrating neurons is significant statistically compared to controls (no EF). (*$P < 0.01$). [Color figure can be viewed in the online issue which is available at www.interscience.wiley.com.]**

no EF stimulation and in neurons subjected to EF stimulation. Most neurons stimulated with EFs showed cathodal asymmetry with strong staining of MAP-2 in the cathode-facing neurites (Fig. 6A).

The distribution of MAP-2 was determined by linescan and fluorescent intensity analysis using Metamorph software. The

linescan measurement was performed along the cell axis. The cell could be artificially divided into the left (anodal) and right (cathodal) half centered at the nucleolus. Most neurites fall in either the left or the right half. The fluorescent intensity for the neurites in the left or right half was compared. Both asymmetric distribution and symmetric distribution of MAP-2 have been seen in cultured neurons without EF stimulation (total cell number, 79) (Fig. 6B). Figure 6B also showed the asymmetric distribution of MAP-2 in neurons subjected to an applied EF (total cell number, 83). 60.6% ± 1.6% of EF-exposed neurons showed cathodal asymmetry of MAP-2, which is significantly higher than control neurons with no EF stimulation (35.6% ± 4.0%, $P < 0.01$) and than neurons showing anodal asymmetry in the EF (22% ± 1.2%, $P < 0.01$) (Fig. 6C). Interestingly, the neuron with an axis perpendicular to the EF also showed biased MAP-2 distribution with the higher fluorescent intensity at the cathode-facing side (Fig. 6B 4). In conclusion, the proportion of neurons showing asymmetry of MAP-2 staining increased substantially in EF-exposed neurons and the asymmetry was biased toward the cathode.

### Growth Cone Reorientation Directs Neuron Migration and Is Time- and Voltage-Dependent

Figure 7 shows time lapse images of growth cone reorientations at 0, 20, 40, and 60 min. Most neurons at 0 min were bipolar in shape with an extended growth cone at the leading process. To show the direction of the leading process, lines were drawn from the starting point of the neurite at the cell soma to the middle of the growth cone. The direction of the leading process was labeled with arrows (Fig. 7D). Different colored arrowheads indicate the location of individual neurons in each frame. After 60 min in the EF (200 mV/mm), most leading neurites faced the cathode (Figs. 7A–C). The neurite orientation index showed that the orientation of the leading process was time- and voltage-dependent (Figs. 7E,F). At a field strength of 50 mV/mm, the orientation index did not show any significant increase during 60-min EF stimulation. The orientation index increased gradually at 120 mV/mm and was significantly higher by 60 min compared with 0 min ($P < 0.05$). The orientation index was field-strength dependent and increased continuously in EF of 200 and 300 mV/mm.

By analyzing the changes in neurite orientation and neuronal migration directedness when the EF direction was reversed, we were able to demonstrate conclusively that EF-induced neurite reorientation determined EF-directed neuronal migration. The migration of three neurons was tracked and analyzed (Figs. 8A,B). The relative relation of growth cones to cell bodies are shown in diagrammatic form in Figure 8C. The green and yellow shapes represent the growth cone and cell body, respectively. Growth cones (green) are located in front of the cell body (they are shown detached from it) and guide the direction of migration of the cell body. When the EF vector is reversed, growth cones change migration direction first, and this is followed by a redirected migration of the cell body.

### Neurons Use Different Strategies to Change Their Direction of Migration

We studied the manner of neurite reorientation when an EF was applied (total cell number = 73) and when the EF polarity was reversed (total cell number = 70). With no applied EFs, neuronal migration was directed randomly. Neurons changed their migration direction in three ways; by branching of the leading growth cone, by turning of the leading process, or by swapping over leading and trailing processes (Fig. 9A). After the EF was switched on, most neurites turned if they were opposite to the cathodal pole. Three typical types of neurite turning were observed in an EF. Type one is where a new neurite formed by branching from the original neurite, and the new neurite subsequently was oriented to face the new cathode. In type two, the neurite turned gradually to the new cathode dragging the cell body in tow. In the third type, the neuron remarkably swapped its leading neurite to face cathodally after EF reversal (Fig. 9B; row 1). The percentage of turning neurites was calculated from the means of three independent experiments at field strength of 200 and 300 mV/mm. These three different types of leading neurite reorientation are shown in diagrammatic form (Fig. 10A). Each type resulted in reoriented steering of neuronal migration and all occurred both in control (randomly directed) neuronal migration and EF-directed neuronal migration. Interestingly, the most common method of changing direction involved a swap of leading process for trailing process when the EF was reversed, with this occurring in more than 50% of cases (Fig. 10B).

## DISCUSSION

Neuronal differentiation involves three sequential stages; cell division and determination, neuronal migration to their final location, and finally differentiation of neuronal axons and dendritic arbors. All three stages are controlled genetically and epigenetically.

Previous work has indicated that electrical cues present in the extracellular spaces may control both neuronal migration and neuronal pathfinding (McCaig et al., 2005; Yao et al., 2008). Here, we demonstrate for the first time electrical control over the axis of neuron-like cell and glial-like cell division. In addition, we show that in an applied EF, the leading neurite, the Golgi apparatus, and the centrosome all redistribute asymmetrically to the cathode-facing side of migrating hippocampal neurons. This cathodal polarization of the leading process occurred before the neurite changed direction and was causal in steering neuronal migration toward the cathode. ROCK and PI3K played an important role in EF-induced Golgi polarization. Pharmacological inhibition of ROCK and PI3K decreased EF-directed leading neurite orientation and Golgi polarization and decreased the directedness of EF-guided neuronal migration.

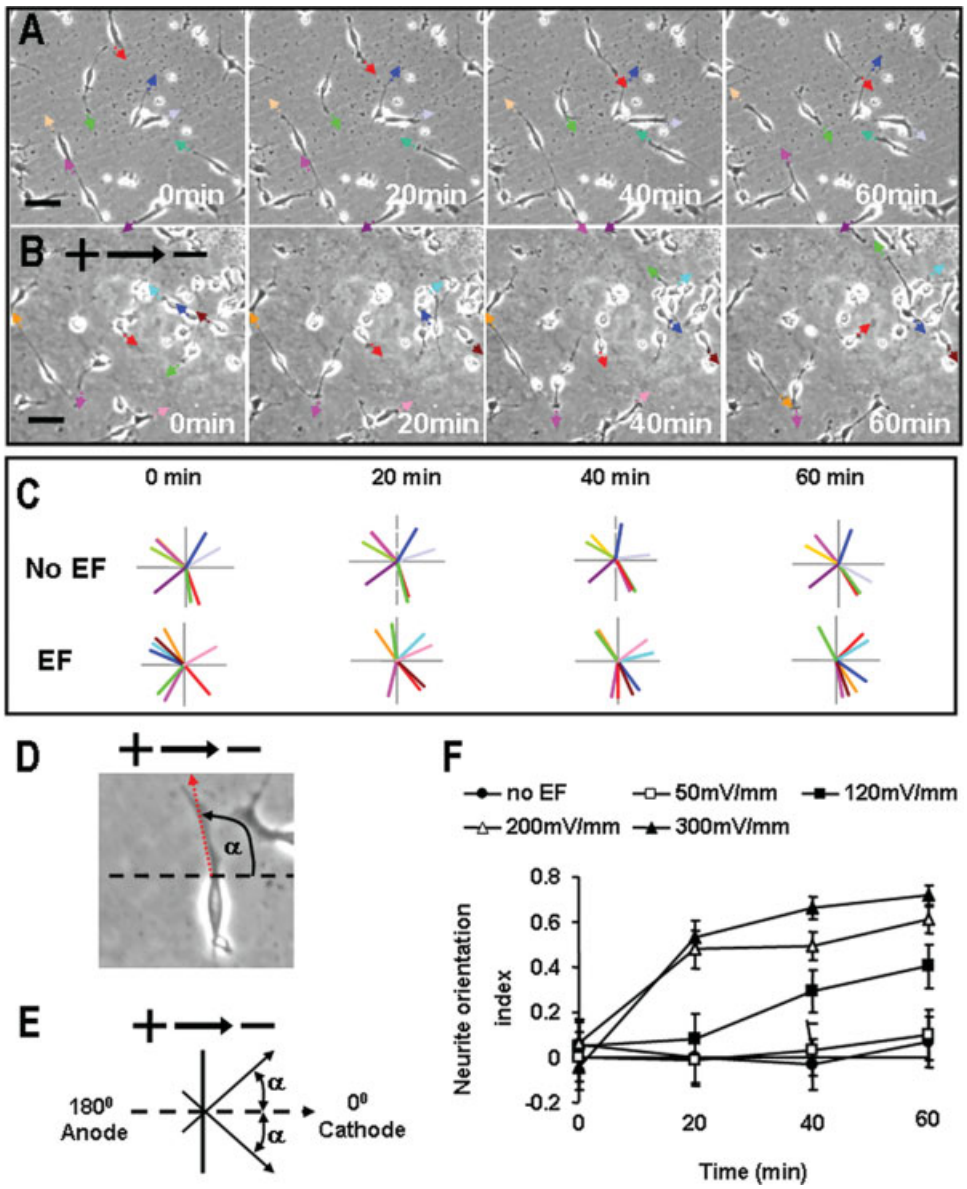


**FIGURE 7. Neurite orientation in EFs. (A, B) Time-lapse images of migrating neurons shown at time points 0, 20, 40, and 60 min. Different colored arrowheads indicate the directions of neuron leading neurites. (A) Without EFs stimulation, neurites oriented and migrated randomly with time. (B) The direction of leading processes gradually changed to face the cathode with time in an EF (200 mV/mm) and by 60 min, most leading neurites faced the cathode. (C) The same directional analysis of neurite orientation of hippocampal neurons described in (A) and (B). Each vector diagram represents the direction of the leading processes of neurons at various time points during the time-lapse experiment. (D) A line is drawn between the point at which the neurite emerged from the soma and the center of the growth cone to show the direction of the leading process. The angle between this line and the EF vector (dashed line) was measured. (E) Schematic diagram shows the quantification method of neurite orientation (see Methods). (F) Time- and voltage-dependent leading neurite orientation of migrating neurons in EFs. Scale bar: 50 μm. [Color figure can be viewed in the online issue which is available at www.interscience.wiley.com.]**

## Small Electrical Signals Oriented the Axis of Division of Hippocampal Cells

When cultured human corneal epithelial cells were exposed to an EF of physiological magnitude, cells divided with a cleavage plane perpendicular to the EF vector (Zhao et al., 1999). In vivo experiments also have shown that a wound-induced EF controls the orientation of the axis of cell division; most epithelial cells divided with a cleavage plane parallel to the wound edge and perpendicular to the EF vector (Song et al., 2002). Neurogenesis and neuronal cell divisions occur postnatally in the hippocampus of several species, including rat, mouse, rabbit, guinea pig, and cat (Altman and Das, 1965, 1967; Caviness, 1973; Gueneau et al., 1982). Here, we show that division of MAP2 and GFAP-labeled presumptive neurons and glia are also strongly directed by an applied EF: the cleavage furrow

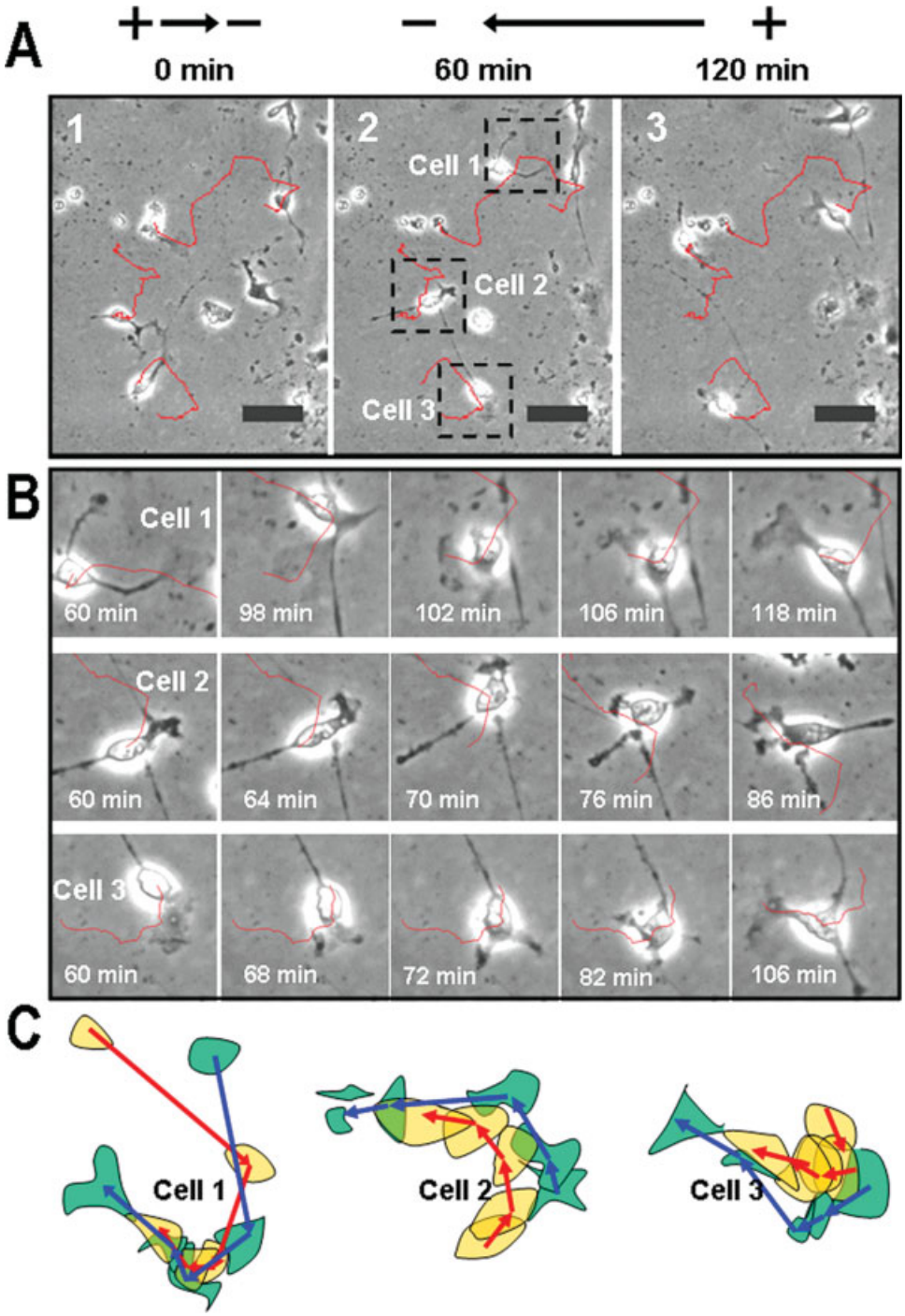


**FIGURE 8.** Growth cone orientation leads to neuronal migration in EFs. (A) Tracks of neuronal migration. Neurons migrated toward the cathode in an EF and migrated to the new cathode when the EF vectors were reversed. The tracks of neuronal migration are labeled with red lines. Plate A2 shows the cells at the end of its initial cathodal migration. This is also the start point of the new migration immediately after the EF direction was reversed. (B) The migration of the three neurons (Cells 1, 2, and 3 from Fig. 8A above) in EFs during the migration stage between A2 and A3 (EF reversed). The first column of the images showed the same state of the cells in Figure 8A2. It is the time point that the EF vectors were switched. When neurons migrate in EFs, the leading processes guide the direction of neuronal migration. (C) Outlines of cell bodies (yellow) and growth cones (green) of the three migrating neurons (shown in rows in B) show that growth cone reorientation leads the way for neuron cell body movement. Growth cones migrate in front of the cell body and their reorientation redirects cell body migration. The paths followed by the growth cones are outlined by blue lines and the paths followed by the cell bodies are outlined by red lines At each stage, the cathodal reorientation of the blue line (growth cones) is more pronounced than that of the red lines (the cell bodies). [Color figure can be viewed in the online issue which is available at www.interscience.wiley.com.]

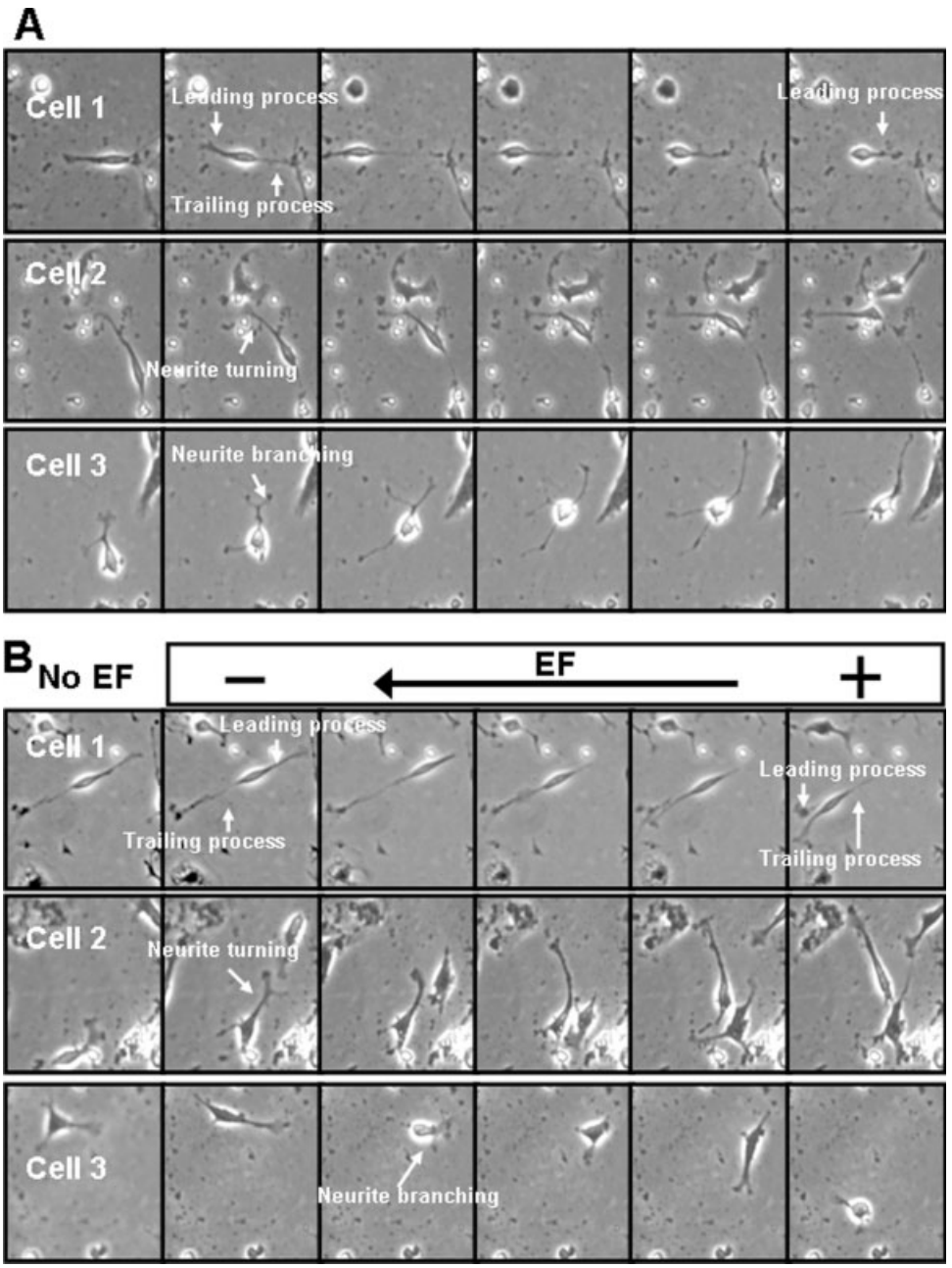


**FIGURE 9. Manner of neurite orientation in EFs. (A) Types of neurite reorientation without EF stimulation. Three types of neurite orientation during randomly directed migration over 1 h. Cell 1, cell 2, and cell 3 (shown in rows) reoriented migration by neurite branching, neurite turning, and neurites swapping between leading and trailing processes, respectively. Time interval between images is 10 min. (B) Types of neurite orientation with EFs stimulation. Three typical types of neurite reorientation of migrating neurons after EFs were switched on. Top row, after EFs were switched on, the leading neurite and trailing neurite of cell 1 swapped orientation; middle row, the leading neurite of cell 2 turned gradually to the cathode; bottom row, a new neurite on cell 3 formed after it branched from the original neurite, the new neurite subsequently oriented to face the cathode. Time interval between images is 10 min. Scale bar: 30 μm.**

lies perpendicular and the mitotic spindle parallel to the EF vector. There are many instances in which brain activity gives rise to significant extracellular EFs. Endogenous EFs around 50 mV/mm have been recorded during evoked potentials from hippocampal granule cells and can persist for minutes to hours (Lomo, 1971). Synchronous firing of action potentials in models of epilepsy give rise to steady voltage gradients of between 10 and 50 mV/mm in extracellular spaces (Jefferys, 1981) and traumatic wounding to the brain, also has been shown to induce DC EF that persist for many hours (Reid et al., 2007).

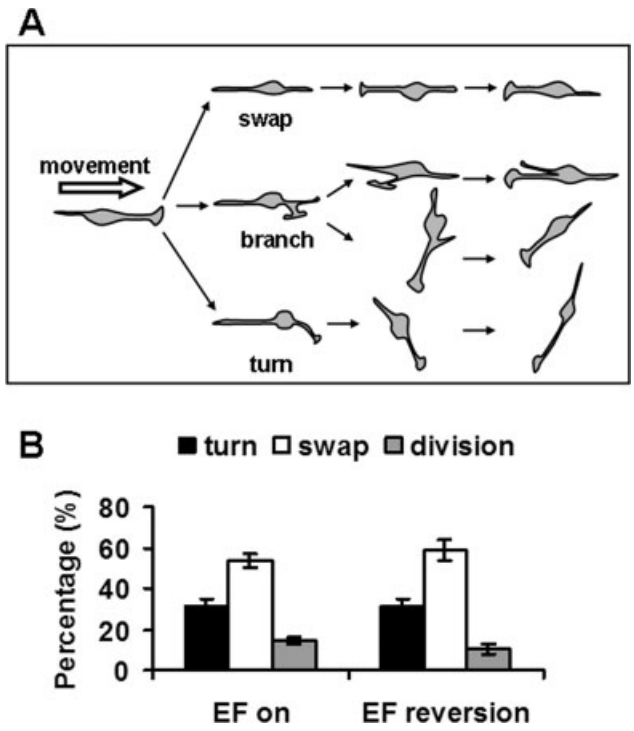


**FIGURE 10. Leading neurite reorientation steers neuronal migration. (A) The drawings illustrate three types of representative leading processes reorientation, namely swapping over of leading and trailing processes, leading neurite branching, and leading neurite turning. These occurred both during random neuronal migration and neuronal migration in an applied EF. (B) Quantitative analysis of the types of neurite reorientation in EFs. The percentage of leading neurite reorientation was calculated from experiments using EFs of 200 and 300 mV/mm.**

## Cathodal Polarization of Neuronal Morphology by an Applied EF

EFs also induce cell polarization and direct cell migration. For example, amoebae react to switching off or reversal of the direction of the DC EF by distinct changes in their shape within a second (Korohoda et al., 2000). The formation of new pseudopodia started at the cathode-facing side and was prevented at the anode-facing side. CHO cells stimulated with EFs, also polarized with distinct lamellipodia facing the cathode (Pu and Zhao, 2005) and endothelial cells oriented perpendicular to the EFs (Zhao et al., 2004). Here, we found that when an applied EF was switched on, and when it was reversed, the growth cones of neurites not initially facing the cathode pole reoriented to face cathodally.

In one previous study (Rajnicek et al., 1992), after 24-h exposure to an applied EF, embryonic rat hippocampal neurons oriented perpendicular to EFs, but no obvious cathodal migration was observed. In contrast, most dissociated neurones in this short-term study showed a dynamic bipolar shape with short leading and trailing processes typical of migrating neurones. Within 1 h of EF stimulation, neurites showed distinct cathodal polarization. To reorient dynamically in response to an applied EF, neurites most commonly swap over the trailing for the leading process although in fewer instances growth cone turning, or branching were used to reset the direction of cell migration. In line with models for EF-directed cell migration (McCaig et al., 2005), we hypothesize that an as yet unknown, mobile receptor in the membrane becomes translocated to the leading cathodal edge to begin the cascade of intracellular events that leads to setting the direction of migration.

## An Applied EF Polarizes Golgi and Centrosomes in Migrating Neurons

Polarization of the Golgi apparatus can help supply membrane components to the leading edge for membrane protrusion. Signals from the Golgi matrix allow reorientation of the Golgi in the direction of movement (Mellor, 2004). MTs form a peri-nuclear cage-like structure converging into the centrosome and projecting into the leading process from the centrosome. In neurons, the leading process steers migration and the Golgi-centrosome is located at the base of the leading process (Hayashi et al., 2003).

In CHO cells, Golgi polarization and cell migration are oriented by an EF vector and Golgi polarization reinforces and maintains electrically directed cell migration (Pu and Zhao, 2005). Similarly in neurons, we have shown that Golgi and centrosome are polarized by the EF in the same direction as the reoriented leading neurite and the subsequent direction of neuronal migration. The EF-directed neuronal migration is accompanied by the establishment of cathodal polarization of both leading process morphology and intracellular structure, although the detailed temporal relationship of these events is unclear.

## Electric Field-Induced Golgi Polarization and Neurite Orientation Involve PI3K and ROCK Signaling

PI3K is required for Golgi polarization in the migration direction of fibroblast cells (Haugh et al., 2000). Wortmannin (an inhibitor of PI3K) abolished EF-induced Golgi polarization and the polarized changes of morphology of CHO cells (Pu and Zhao, 2005). Rho family members of small GTPases are also important for cell polarity establishment (Nobes and Hall, 1999; Etienne-Manneville and Hall, 2001, 2003; Wojciak-Stothard and Ridley, 2003). Rho is involved in neurite extension and axon formation (Hirose et al., 1998; Katoh et al., 1998; Bito et al., 2000). Here, we demonstrated that LY294002 and Y27632 decreased EF-induced orientation of leading process morphology and Golgi polarization, indicating that Rho and PI3K are involved in EF-directed neurite and Golgi polarization.

This study demonstrates that the migration direction of rat hippocampal neurons can be controlled by EFs. To achieve this, leading process morphology and intracellular structures (Golgi apparatus, centrocsome, MAP-2) all become polarized in the same direction and EF-directed neuron migration ensues. Rho-associated coiled-coil forming protein kinases (ROCK) and phosphatatidylinositol 3-kinase (PI3K) are important regu-

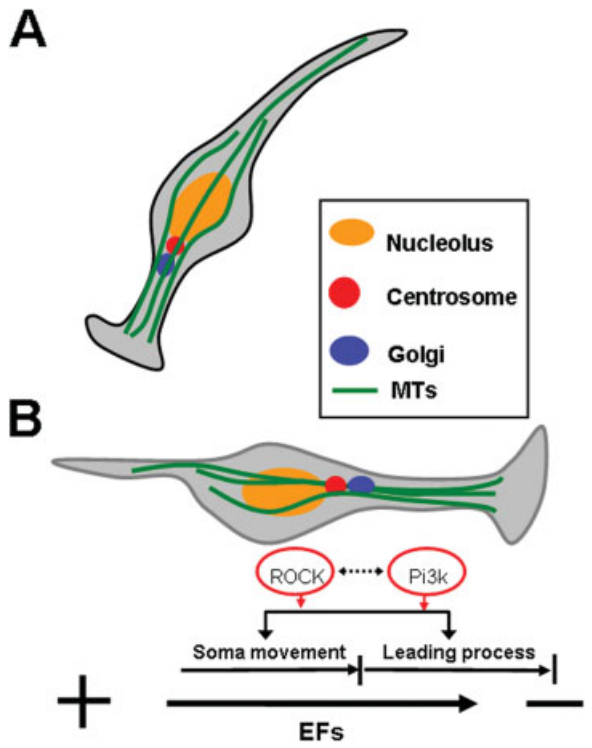


**FIGURE 11. Hippocampal neurons polarize and migrate cathodally in EFs. (A) A randomly migrating neuron. The Golgi apparatus and centrosome are located at the base of the leading neurite. (B) Diagrammatic representation of growth cone of leading process, Golgi apparatus, and centrosome polarized cathodally by an applied EF. The cathodal polarization of neurons occurs in parallel with and may drive the directedness of cathodal neuronal migration. ROCK and PI3K mediate leading neurite orientation, Golgi polarization, and cathodal neuronal migration in EFs. [Color figure can be viewed in the online issue which is available at www.interscience.wiley.com.]**

lators of EFs guided neuron migration (Yao et al., 2008) (Fig. 11).

Previous studies have shown that interactions between Rho and PI3K regulate the organization of cytoskeleton (Bishop and Hall, 2000; Cantrell, 2001). The PI3K signaling cascade is linked by members of one family of GEFs to Rho and Rac activation (Cantrell, 2001; Huang and Reichardt, 2001). In PC12 cells, Rac and Rho are both involved in the PI3K-regulated neurite outgrowth (Kita et al., 1998). In this study, we showed that both ROCK and PI3K play important role in the EFs-directed neurite orientation and the polarization of neuronal organelles. EF-guided neurite orientation and neuron migration may provide a useful model to investigate further the signaling pathway of PI3K and Rho GTPase family in regulating the activity of neuronal cytoskeleton.

Steady DC EFs arise in the central nervous system following focal seizures, local ischemia, and traumatic brain injury. Fields of around 50 mV/mm have been recorded (Jefferys, 1995). In many cases, endogenous neuronal stem cells migrate toward such injury sites in response to the lesion (Sundholm-Peters et al., 2005). The extent to which this is driven by the endogenous electrical signals arising on brain damage remains to be determined. In addition, DC EFs also exist in places where active neurogensis is occurring. For example, a steady voltage gradient of several 100 mV/mm persists across the neural tube in amphibian embryos during periods of neuronal polarization and migration (Hotary and Robinson, 1991). The existence of DC EFs during critical periods of brain development and brain injury raises novel concepts. Since neuronal division, neuronal migration, and neuronal axonal guidance all are regulated by a DC EF, collectively this offers substantial scope for an applied EF (which need not be physiological), or a wound-induced EF to act as a robust guidance cue to direct implanted neurons in efforts to promote CNS repair.

## REFERENCES

Altman J, Das GD. 1965. Autoradiographic and histological evidence of postnatal hippocampal neurogenesis in rats. J Comp Neurol 124:319–335.

Altman J, Das GD. 1967. Postnatal neurogenesis in the guinea-pig. Nature 214:1098–1101.

Bellion A, Baudoin JP, Alvarez C, Bornens M, Metin C. 2005. Nucleokinesis in tangentially migrating neurons comprises two alternating phases: Forward migration of the Golgi/centrosome associated with centrosome splitting and myosin contraction at the rear. J Neurosci 25:5691–5699.

Bishop A, Hall A. 2000. Rho GTPases and their effector proteins. Biochem J 348:241–255.

Bito H, Furuyashiki T, Ishihara H, Shibasaki Y, Ohashi K, Mizuno K, Maekawa M, Ishizaki T, Narumiya S. 2000. A critical role for a Rho-associated kinase, p160ROCK, in determining axon outgrowth in mammalian CNS neurons. Neuron 26:431–441.

Bradke F, Dotti CG. 2000. Establishment of neuronal polarity: Lessons from cultured hippocampal neurons. Curr Opin Neurobiol 10:574–581.

Cantrell D. 2001. Phosphoinositide 3-kinase signaling pathways. J Cell Sci 114:1439–1445.

Catalano SM, Shatz CJ. 1998. Activity-dependent cortical target selection by thalamic axons. Science 281:559–562.

Causeret F, Hidalgo-Sanchez M, Fort P, Backer S, Popoff MR, Gauthier-Rouviere C, Bloch-Gallego E. 2004. Distinct roles of Rac1/Cdc42 and Rho/Rock for axon outgrowth and nucleokinesis of precerebellar neurons toward netrin 1. Development 131:2841–2852.

Caviness VS. 1973. Time of neuron origin in the hippocampus and dentate gyrus of normal and reeler mutant mice: An autoradiographic analysis. J Comp Neurol 151:113–120.

Chenn A, McConnell SK. 1995. Cleavage orientation and the asymmetric inheritance of Notch1 immunoreactivity in mammalian neurogenesis. Cell 25:631–641.

Dantzker JL, Callaway EM. 1998. The development of local, layer-specific visual cortical axons in the absence of extrinsic influences and intrinsic activity. J Neurosci 18:4145–4154.

Dotti CG, Sullivan CA, Banker GA. 1988. The establishment of polarity by hippocampal neurons in culture. J Neurosci 8:1454–1468.

Edmondson JC, Hatten ME. 1987. Glial-guided granule neuron migration in vitro: A high-resolution time-lapse video microscopic study. J Neurosci 7:1928–1934.

Etienne-Manneville S, Hall A. 2001. Integrin-mediated activation of Cdc42 controls cell polarity in migrating astrocytes through PKCzeta. Cell 106:489–498.

Etienne-Manneville S, Hall A. 2003. Cdc42 regulates GSK-3β and adenomatous polyposis coli to control cell polarity. Nature 421:753–756.

Fukata M, Nakagawa M, Kaibuchi K. 2003. Roles of Rho-family GTPases in cell polarisation and directional migration. Curr Opin Cell Biol 15:590–597.

Gasser UE, Hatten ME. 1990. Neuron-glia interactions of rat hippocampal cells in vitro: Glial-guided neuronal migration and neuronal regulation of glial differentiation. J Neurosci 10:1276–1285.

Gueneau G, Privat A, Drouet J, Court L. 1982. Subgranular zone of the dentate gyrus of young rabbits as a secondary matrix. A high-resolution autoradiographic study. Dev Neurosci 5:345–358.

Hannigan M, Zhan L, Li Z, Ai Y, Wu D, Huang CK. 2002. Neutrophils lacking phosphoinositide 3-kinaseγ show loss of directionality during *N*-formyl-Met-Leu-Phe-induced chemotaxis. Proc Natl Acad Sci USA 99:3603–3608.

Haugh JM, Codazzi F, Teruel M, Meyer T. 2000. Spatial sensing in fibroblasts mediated by 3′ phosphoinositides. J Cell Biol 151: 1269–1280.

Hayashi K, Kawai-Hirai R, Harada A, Takata K. 2003. Inhibitory neurons from fetal rat cerebral cortex exert delayed axon formation and active migration in vitro. J Cell Sci 116:4419–4428.

Hinkle L, McCaig CD, Robinson KR. 1981. The direction of growth of differentiating neurons and myoblasts from frog embryos in an applied electric field. J Physiol 314:121–135.

Hirose M, Ishizaki T, Watanabe N, Uehata M, Kranenburg O, Moolenaar WH, Matsumura F, Maekawa M, Bito H, Narumiya S. 1998. Molecular dissection of the Rho-associated protein kinase (p160ROCK)-regulated neurite remodeling in neuroblastoma N1E-115 cells. J Cell Biol 141:1625–1636.

Hotary KB, Robinson KR. 1991. The neural tube of the *Xenopus* embryo maintains a potential difference across itself. Dev Brain Res 59:65–73.

Huang E, Reichardt L. 2001. Neurotrophins: Roles in neuronal development. Annu Rev Neurosci 24:677–736.

Jaffe LF, Poo MM. 1979. Neurites grow faster towards the cathode than the anode in a steady field. J Exp Zool 209:115–128.

Jefferys JGF. 1995. Nonsynaptic modulation of neuronal activity in the brain: Electric currents and extracellular ions. Physiol Rev 75:689–723.

Jefferys JGR. 1981. Influence of electrical fields on the excitability of granule cells in guinea-pig hippocampal slices. J Physiol 319:143–152.

Katoh H, Aoki J, Yamaguchi Y, Kitano Y, Ichikawa A, Negishi M. 1998. Constitutively active Galpha12, Galpha13, and Galphaq induce Rho-dependent neurite retraction through different signaling pathways. J Biol Chem 273:28700–28707.

Kita Y, Kimura K, Kobayashi M, Ihara S, Kaibuchi K, Kuroda S, Ui M, Iba H, Konishi H, Kikkawa U, Nagata S, Fukui Y. 1998. Microinjection of activated phosphatidylinositol-3 kinase induces process outgrowth in rat PC12 cells through the Rac-JNK signal transduction pathway. J Cell Sci 111:907–915.

Korohoda W, Mycielska M, Janda E, Madeja Z. 2000. Immediate and long-term galvanotactic responses of Amoeba proteus to dc electric fields. Cell Motil Cytoskeleton 45:10–26.

Kwei SL, Clement A, Faissner A, Brandt R. 1998. Differential interactions of MAP2, tau and MAP5 during axogenesis in culture. Neuroreport 9:1035–1040.

Lomo T. 1971. Patterns of activation in a monosynaptic cortical pathway: The perforant path input to the dentate area of the hippocampal formation. Exp Brain Res 12:18–45.

McCaig CD. 1986a. Dynamic aspects of amphibian neurite growth and the effects of an applied electric field. J Physiol 375:55–69.

McCaig CD. 1986b. Electric fields, contact guidance and the direction of nerve growth. J Embryol Exp Morphol 94:245–255.

McCaig CD. 1987. Spinal neurite reabsorption and regrowth in vitro depend on the polarity of an applied electric field. Development 100:31–41.

McCaig CD, Allan DW, Erskine L, Rajnicek AM, Stewart R. 1994. Growing nerves in an electric field. Neuroprotocols 4:134–141.

McCaig CD, Rajnicek AM, Song B, Zhao M. 2005. Controlling cell behavior electrically: Current views and future potential. Physiol Rev 85:943–978.

Mellor H. 2004. Cell motility: Golgi signalling shapes up to ship out. Curr Biol 14:434–435.

Miyata S, Matsumoto N, Maekawa S. 2003. Polarized targeting of IgLON cell adhesion molecule OBCAM to dendrites in cultured neurons. Brain Res 979:129–136.

Nobes CD, Hall A. 1999. Rho GTPases control polarity, protrusion, and adhesion during cell movement. J Cell Biol 144:1235–1244.

Pu J, Zhao M. 2005. Golgi polarization in a strong electric field. J Cell Sci 118:1117–1128.

Rajnicek AM, Gow NA, McCaig CD. 1992. Electric field-induced orientation of rat hippocampal neurones in vitro. Exp Physiol 77: 229–232.

Rajnicek AM, Foubister LE, McCaig CD. 2006. Temporally and spatially coordinated roles for rho, rac, cdc42 and their effectors in growth cone guidance by a physiological electric field. J Cell Sci 119:1723–1734.

Reid B, Nuccitelli R, Zhao M. 2007. Non-invasive measurement of bioelectric currents with a vibrating probe. Nat Protoc 2:661–669.

Rickmann M, Amaral DG, Cowan WM. 1987. Organization of radial glial cells during the development of the rat dentate gyrus. J Comp Neurol 264:449–479.

Shi R, Borgens RB. 1995. Three-dimensional gradients of voltage during development of the nervous system as invisible coordinates for the establishment of embryonic pattern. Dev Dyn 202:101–114.

Song B, Zhao M, Forrester JV, McCaig CD. 2002. Electrical cues regulate the orientation and frequency of cell division and the rate of wound healing in vivo. Proc Natl Acad Sci USA 99:13577–13582.

Sundholm-Peters NL, Yang HK, Goings GE, Walker AS, Szele FG. 2005. Subventricular zone neuroblasts emigrate toward cortical lesions. J. Neuropathol Exp Neurol 64:1089–1100.

Tanaka T, Serneo FF, Higgins C, Gambello MJ, Wynshaw-Boris A, Gleeson JG. 2004. Lis1 and doublecortin function with dynein to mediate coupling of the nucleus to the centrosome in neuronal migration. J Cell Biol 165:709–721.

Ward M, McCann C, DeWulf M, Wu JY, Rao Y. 2003. Distinguishing between directional guidance and motility regulation in neuronal migration. J Neurosci 23:5170–5177.

Wojciak-Stothard B, Ridley AJ. 2003. Shear stress-induced endothelial cell polarization is mediated by Rho and Rac but not Cdc42 or PI 3-kinases. J Cell Biol 161:429–439.

Yacubova E, Komuro H. 2002. Intrinsic program for migration of cerebellar granule cells in vitro. J Neurosci 22:5966–5981.

Yao L, Shanley L, McCaig C, Zhao M. 2008. Small applied electric fields guide migration of hippocampal neurons. J Cell Physiol 216:527–535.

Zhao M, Agius-Fernandez A, Forrester JV, McCaig CD. 1996. Orientation and directed migration of cultured corneal epithelial cells in small electric fields are serum dependent. J Cell Sci 109:1405–1414.

Zhao M, Forrester JV, McCaig CD. 1999. A small, physiological electric field orients cell division. Proc Natl Acad Sci USA 96:4942–4946.

Zhao M, Pu J, Forrester JV, McCaig CD. 2002. Membrane lipids, EGF receptors and intracellular signals co-localize and are polarized in epithelial cells moving directionally in a physiological electric field. FASEB J 16:857–859.

Zhao M, Bai H, Wang E, Forrester JV, McCaig CD. 2004. Electrical stimulation directly induces pre-angiogenic responses in vascular endothelial cells by signaling through VEGF receptors. J Cell Sci 117:397–405.